International Journal of Bifurcation and Chaos, Vol. 15, No. 12 (2005) 4051–4063

STATE SPACE RECONSTRUCTION USING EXTENDED STATE OBSERVERS TO CONTROL CHAOS IN A NONLINEAR PENDULUM

FRANCISCO HEITOR I. PEREIRA-PINTO and ARMANDO M. FERREIRA
Instituto Militar de Engenharia,
Department of Mechanical and Materials Engineering,
22.290.270, Rio de Janeiro, Brazil

MARCELO A. SAVI
Universidade Federal do Rio de Janeiro,
COPPE — Department of Mechanical Engineering,
21.941.972, Rio de Janeiro, P.O. Box 68.503, Brazil
savi@ufrj.br

Received July 12, 2004; Revised January 3, 2005

Chaos control may be understood as the use of tiny perturbations for the stabilization of unstable periodic orbits embedded in a chaotic attractor. Since chaos may occur in many natural processes, the idea that chaotic behavior may be controlled by small perturbations of some physical parameter allows this kind of behavior to be desirable in different applications. In general, it is not necessary to have a mathematical model to achieve the control goal since all control parameters may be resolved from time series analysis. Therefore, state space reconstruction is an important task related to chaos control. This contribution analyzes chaos control performed using a semi-continuous method based on OGY approach and proposes the use of extended state observers in order to perform state space reconstruction. The use of extended state observers allows a direct application of the control method. Comparing with the delay coordinates method, extended state observers avoids the calculation of parametric changes related to delayed Poincaré sections that influence the system dynamics. The proposed procedure is applied in the control of chaos in a nonlinear pendulum, showing that it may be used to control chaos in mechanical systems.

Keywords: Chaos; control; time series; state space reconstruction; nonlinear pendulum.

1. Introduction

Chaos control is based on the richness of responses of chaotic behavior. A chaotic attractor has a dense set of unstable periodic orbits (UPOs) and the system often visits the neighborhood of each one of them. Moreover, chaotic response has sensitive dependence to initial condition, which implies that the system's evolution may be altered by small perturbations. Therefore, chaos control may be understood as the use of tiny perturbations for the stabilization of an UPO embedded in a chaotic attractor, which allows this kind of behavior to be desirable in a variety of applications, since one of these UPOs can provide better performance than others in a particular situation.

The experimental analysis of nonlinear dynamical systems furnishes a scalar sequence of measurements, which may be analyzed using state space reconstruction and other techniques related to nonlinear analysis. The basic idea of the state space

reconstruction is that a signal contains information about unobserved state variables that can be used to predict the present state. Basically, there are two ways of addressing this general problem: one employs delay coordinate embedding technique while the other uses the derivative coordinates technique [Packard *et al.*, 1980; Takens, 1981; Broomhead & King, 1986; Ruelle, 1979]. Therefore, a scalar time series may be used to construct a vector time series that is equivalent to the system dynamics from a topological point of view.

Recently, tools usually related to control theory are being employed in the analysis of chaotic behavior. Among others, one could mention extended state observers (ESO) for the determination of nonobserved state of a dynamical system [So *et al.*, 1994; Ramirez & Villamil, 1995; Femat *et al.*, 1997; Cao, 2000; Bowong & Kakmeni, 2003].

The main purpose of this contribution is the use of extended state observers to perform state space reconstruction in order to be applied to chaos control in a nonlinear pendulum. This pendulum has both torsional stiffness and damping and was previously analyzed by Franca and Savi [2001] and Pinto and Savi [2003]. Pereira-Pinto *et al.* [2004] considered the chaos control of the cited pendulum using the close-return (CR) method [Auerbach *et al.*, 1987] to determine the UPO embedded in the attractor, and a variation of the OGY technique called semi-continuous control (SCC) method, proposed firstly by Hübinger *et al.* [1994] and extended by Korte *et al.* [1995]. All signals are generated numerically by the integration of the mathematical model equations, which uses experimentally identified parameters. The cited article analyzes the chaos control considering the analysis with either all state variables or just a single scalar time series are available. When a single time series is available, state space reconstruction is done employing delay coordinates method. Here, the control analysis considers that only a scalar time series is available and the state space reconstruction is done by the use of extended state observers. Results show the potentiality of the use of ESO for state space reconstruction, especially when chaos control is of concern.

2. Chaos Control Method

The control of chaos can be treated as a two-stage process. The first stage is composed by the identification of UPO and is named as "learning stage". Since UPO are system invariants, they can be analyzed from state space reconstructed from a scalar time series [Gunaratne *et al.*, 1989].

This article considers the close-return (CR) method [Auerbach *et al.*, 1987] for the detection of UPO embedded in the attractor. The basic idea is to search for a period-P UPO in the time series represented by vectors $\{u_i\}_{i=1}^{N}$. The identification of a period-P UPO is based on a search for pairs of points in the time series that satisfy the condition $|u_i - u_{i+P}|_{i=1}^{(N-P)} \leq r_1$ where r_1 is the tolerance value for distinguishing return points. After this analysis, all points that belong to a period-P cycle are grouped together. During the search, the vicinity of a UPO may be visited many times, and it is necessary to distinguish each orbit, remove any cycle permutation and to average them in order to improve estimations as shown by Otani and Jones [1997].

After the identification of a UPO, one can proceed to the next stage of the control process that is the stabilization of the desired orbit. Chaos control methods may be classified as discrete or continuous techniques. The first chaos control method had been proposed by Ott *et al.* [1990], nowadays known as the OGY (Ott–Grebogi–Yorke) method. On the other hand, continuous methods are exemplified by the so-called delayed feedback control, proposed by Pyragas [1992], which states that chaotic systems can be stabilized by a feedback perturbation proportional to the difference between the present and a delayed states of the system.

The OGY [Ott *et al.*, 1990] approach is described considering a discrete system of the form of a map $\xi_{i+1} = F(\xi_i, p)$, where $p \in \Re$ is an accessible parameter for control. This is equivalent to a parameter dependent map associated with a general surface, usually a Poincaré section. Let $\xi_F = F(\xi_F, p_0)$ denote the unstable fixed point on this section corresponding to an orbit in the chaotic attractor that one wants to stabilize. Basically, the control idea is to monitor the system dynamics until the neighborhood of this point is reached. After that, a proper small change in the parameter p causes the next state ξ_{i+1} to fall into the stable direction of the fixed point.

The semi-continuous control (SCC) method [Hübinger *et al.*, 1994] lies between the continuous and the discrete time control. This introduces as many intermediate Poincaré sections, viewed as control stations, as it is necessary to achieve stabilization of a desirable UPO. Therefore, the SCC

method is based on measuring transition maps of the system and provides a more effective control, necessary for systems with large instability orbits, for example. These maps relate the state of the system in one Poincaré section to the next. In order to use N control stations per forcing period T, one introduces N equally spaced successive Poincaré sections Σ_n, $n = 0, \ldots, (N-1)$. Let $\xi_F^n \in \Sigma_n$ be the intersections of the UPO with Σ_n and $F^{(n,n+1)}$ be the mapping from one control station Σ_n to the next one Σ_{n+1}. Hence, one considers the map

$$\xi_F^{n+1} = F^{(n,n+1)}(\xi_F^n, p^n). \tag{1}$$

A linear approximation of $F^{(n,n+1)}$ around ξ_F^n and p_0 is considered as follows:

$$\delta\xi^{n+1} \cong A^n \delta\xi^n + w^n \delta p^n, \tag{2}$$

where $\delta\xi^{n+1} = \xi^{n+1} - \xi_F^{n+1}$, $\delta p^n = p^n - p_0$, $A^n = D_{\xi^n} P^{(n,n+1)}(\xi_F^n, p_0)$, and $w^n = (\partial P^{(n,n+1)}/\partial p^n)\,(\xi_F^n, p_0)$.

Hübinger *et al.* [1994] analyzed the possibility of the eigenvalues of A^n to be complex numbers and then they used the fact that the linear mapping A^n deforms a sphere around ξ_F^n into an ellipsoid around ξ_F^{n+1}. Therefore, a singular value decomposition (SVD),

$$\begin{aligned} A^n &= U^n W^n (V^n)^T \\ &= \{u_u^n \quad u_s^n\} \begin{bmatrix} \sigma_u^n & 0 \\ 0 & \sigma_s^n \end{bmatrix} \{v_u^n \quad v_s^n\}^T, \end{aligned} \tag{3}$$

is employed in order to determine the directions v_u^n and v_s^n in Σ_n which are mapped onto the largest, $\sigma_u^n u_u^n$, and shortest, $\sigma_s^n u_s^n$, semi-axis of the ellipsoid in Σ_{n+1}, respectively. Here, σ_u^n and σ_s^n are the singular values of A^n.

Korte *et al.* [1995] established the control target as being the adjustment of δp^n such that the direction v_s^{n+1} on the map $n+1$ is obtained, resulting in a maximal shrinking on map $n+2$. Therefore, it demands $\delta\xi^{n+1} = \alpha v_s^{n+1}$, where $\alpha \in \Re$. Hence, from Eq. (2) one has that

$$A^n \delta\xi^n + w^n \delta p^n = \alpha v_s^{n+1}, \tag{4}$$

which is a relation from which α and δp^n can be conveniently chosen.

3. State Space Reconstruction Using Extended State Observers

A state observer may be understood as an auxiliary system that is employed to estimate a nonobserved state [Luenberger, 1964, 1966; Kalman, 1960]. The observer is a very useful tool for receiving information of the variables of a system that are otherwise unknown. For this reason, it is usually employed in control systems where knowledge of the plant system is necessary from an incomplete observation. In general, the use of state observers is related to estimating, controlling and also detecting and identifying failures in dynamical systems.

This contribution uses the idea of extended state observers to promote state space reconstruction. In order to introduce the basic ideas of this procedure, consider a general nonlinear system given by:

$$\begin{cases} \dot{x}_1 = x_2 \\ \dot{x}_2 = f(x_1, x_2, w(x,t)) + b_0 u(x,t) \\ y = x_1 \end{cases} \tag{5}$$

where f is a nonlinear function that represents the dynamics of the system and the disturbance, $w(x,t)$ is the external unknown input disturbance, $u(x,t)$ is the control signal and y is the observable output. Notice that $y = x_1$ is the only measured variable and the parameter b_0 is known. Therefore, it is necessary to estimate x_2 in order to determine the full state of the system.

Nonlinear systems have many types of uncertainties, such as imperfections of mechanisms, unknown nonlinearities and parameters, which make impossible to obtain an exact function f. Since classical state observer designs, including high-gain and sliding-mode observers, depend on the perfect knowledge of the system dynamics, Han [1995] suggests an alternative method called extended state observer as an approach to deal with the estimation of states of dynamics that do not have a mathematical model. With this aim, the system (5) is augmented as

$$\begin{cases} \dot{x} = Ax + Bu + Eh \\ y = Cx \end{cases} \tag{6}$$

where

$$A = \begin{bmatrix} 0 & 1 & 0 \\ 0 & 0 & 1 \\ 0 & 0 & 0 \end{bmatrix}, \quad B = \begin{Bmatrix} 0 \\ b_0 \\ 0 \end{Bmatrix},$$

$$C = \{1 \quad 0 \quad 0\}, \quad E = \begin{Bmatrix} 0 \\ 0 \\ 1 \end{Bmatrix}$$

Notice that, now, vector x is defined by, $x = \{x_1 \quad x_2 \quad x_3\}^T$, where variable $x_3 = f(x_1, x_2, w(x,t))$ represents an extended state. It should be pointed out that, both f and its derivative $h = \dot{f}$ are unknown. However, by making f as a state, it is now possible to estimate it by using a state observer. Han [1995] proposed the following form for the state observer:

$$\dot{\hat{x}} = A\hat{x} + Bu + LG(e) \tag{7}$$

Here, $\hat{x} = \{\hat{x}_1 \quad \hat{x}_2 \quad \hat{x}_3\}^T$ are estimated values of vector x. Notice that $\hat{x}_3$ represents an estimative of $f(x_1, x_2, w(x,t))$, and $e = x_1 - \hat{x}_1$ represents the error associated with the estimation. Moreover, L is the observer gain vector, which can be obtained using known method such as pole placement method. In this equation, the following vectors are used:

$$L = \{\beta_1 \quad \beta_2 \quad \beta_3\}^T \tag{8}$$

$$G(e) = \{g_1(e) \quad g_2(e) \quad g_3(e)\} \tag{9}$$

The gain of the observer is chosen in order to obtain a good estimative for the system variables. Therefore, function g_i is defined as a modified exponential gain function [Wang & Gao, 2003]:

$$g_i(e, \alpha_i, \delta) = \begin{cases} |e|^{\alpha_i} \operatorname{sign}(e), & |e| > \delta \\ \dfrac{e}{\delta^{1-\alpha_i}}, & |e| \le \delta \end{cases} \tag{10}$$

The parameter δ is a small number used to limit the gain in the neighborhood of the origin. This procedure prevents excessive gain when the error is small avoiding high frequency chattering [Gao *et al.*, 2001]. Therefore, when $0 < \alpha_i < 1$, g_i yields high gain for small errors, $|e| \le \delta$. On the other hand, when $\alpha_i < 0$, a reduction of the observed error occurs.

The definition of the gain is closely related to the dynamics characteristics of the system. Usually, the first trial considers a linear gain ($\alpha_i = 1$, $i = 1, 2, 3$), $g_i(e, \alpha_i, \delta) = e$ ($i = 1, 2, 3$). Under this assumption, the pole placement method can be used for the initial design of this observer. Nonlinearities can be added in order to improve the performance of the observer. Nevertheless, it is important to say that nonlinear gain functions introduce higher complexity in the estimation algorithm [Gao, 2003].

The stability of the observer is assured from an appropriate choice of parameters β_i. The stability of a linear extended state observer can be analyzed subtracting the observer equation (7) from system equation (6). This procedure gives an equation for the error dynamics:

$$\dot{e} = A_e e + Eh \tag{11}$$

where

$$A_e = A - LC = \begin{bmatrix} -\beta_1 & 1 & 0 \\ -\beta_2 & 0 & 1 \\ -\beta_3 & 0 & 0 \end{bmatrix}.$$

The stability of the error dynamics is associated with the roots of the characteristic polynomial of A_e, since h is bounded:

$$\lambda(s) = s^3 + \beta_1 s^2 + \beta_2 s + \beta_3 = 0 \tag{12}$$

In order to tune the linear ESO, the roots must be all in the open left-half. Gao [2003] defines the ω_o-parameterization where all observer eigenvalues must be equal to $-\omega_o$. Therefore, $L = \{\beta_1 \quad \beta_2 \quad \beta_3\}^T$ becomes a function of ω_o, which is denoted as the bandwidth of the observer. Then,

$$\lambda(s) = s^3 + \beta_1 s^2 + \beta_2 s + \beta_3 = (s + \omega_o)^3 = 0 \tag{13}$$

Solving this equation, one obtains the following relationship between β_i and ω_o:

$$\beta_1 = 3\omega_o, \quad \beta_2 = 3\omega_o^2, \quad \beta_3 = \omega_o^3 \tag{14}$$

4. Nonlinear Pendulum

As a mechanical application of the procedures presented in this article, a nonlinear pendulum is considered. The motivation of the proposed pendulum is an experimental set up, previously analyzed by Franca and Savi [2001], Pinto and Savi [2003]. Pereira-Pinto *et al.* [2004] presented a mathematical model to describe the dynamical behavior of the pendulum. Here, just the equations of motion are shown. For more details, see the cited reference.

The considered nonlinear pendulum is shown in Fig. 1. The right-hand side presents the experimental apparatus while the left-hand side shows a schematic picture. Basically, the pendulum consists of an aluminum disc (1) with a lumped mass (2) that is connected to a rotary motion sensor (4). A magnetic device (3) provides an adjustable dissipation of energy. A string-spring device (6) provides torsional stiffness to the pendulum and an electric motor (7) excites the pendulum via the string-spring device. An actuator (5) provides the necessary perturbations to stabilize this system by properly changing the string length.

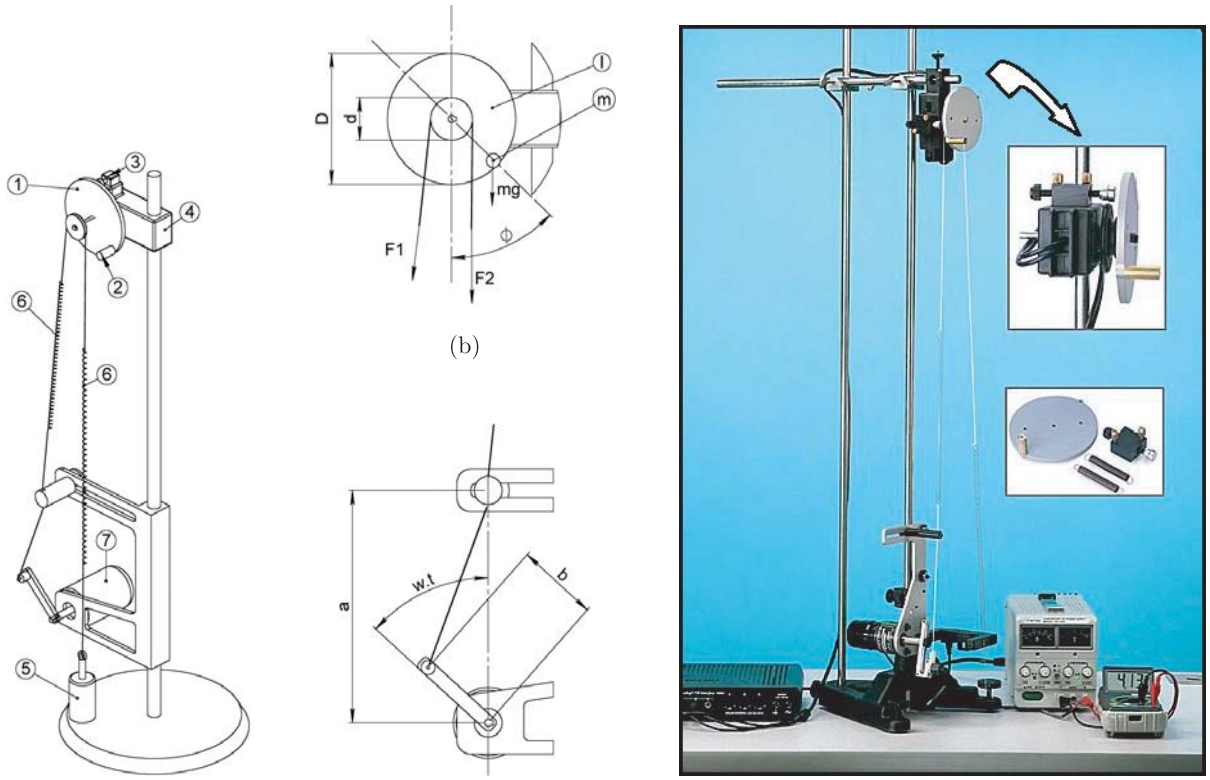

Fig. 1. Nonlinear pendulum. (a) Physical model. (1) Metallic disc; (2) Lumped mass; (3) Magnetic damping device; (4) Rotary motion sensor; (5) Actuator; (6) String-spring device; (7) Electric motor. (b) Parameters and forces on the metallic disc. (c) Parameters from driving device. (d) Experimental apparatus.

The equations of motion of this pendulum is given by [Pereira-Pinto *et al.*, 2004]:

$$\begin{Bmatrix} \dot{\phi} \\ \ddot{\phi} \end{Bmatrix} = \begin{bmatrix} 0 & 1 \\ -\dfrac{kd^2}{2I} & -\dfrac{\zeta}{I} \end{bmatrix} \begin{Bmatrix} \phi \\ \dot{\phi} \end{Bmatrix} + \begin{Bmatrix} 0 \\ \dfrac{kd}{2I}[\sqrt{a^2+b^2-2ab\cos(\varpi t)} - (a-b) - \Delta l] - \dfrac{mgD}{2I}\sin(\phi) \end{Bmatrix} \quad (15)$$

where ϖ is the forcing frequency, a defines the position of the guide of the string with respect to the motor, b is the length of the excitation arm of the motor, D is the diameter of the metallic disc and d is the diameter of the driving pulley; I is the total inertia of rotating parts, m is the lumped mass and ζ is the dissipation parameter. The Δl parameter is the length variation in the string provided by the linear actuator (5) shown in Fig. 1(a). This parameter is considered as the variation on the accessible parameter for control purposes.

The determination of parameters in the equation of motion is done considering the experimental setup of Franca and Savi [2001]. Table 1 shows the parameters that are evaluated from the experimental setup. Moreover, values of the adjustable parameters ϖ and ζ are tuned to generate chaotic response in agreement to the experimental work.

Table 1. Experimental parameters.

a (m)	b (m)	d (m)	D (m)	I (kg m^4)	k (N/m)	m (kg)
1.6×10^{-2}	6.0×10^{-2}	2.9×10^{-2}	9.2×10^{-2}	1.876×10^{-4}	4.736	1.6×10^{-2}

The Δl parameter has a null value for the system without control action. Therefore, using the parameters presented in Table 2, it is possible to use a fourth-order Runge–Kutta scheme in order to perform numerical simulations of the equations of motion. Figure 2 shows temporal evolution, phase space and strange attractor related to this response.

Table 2. Adjustable parameters.

ϖ (rad/s)	ζ (kg · m^2/s)	Δl (m)
5.15	5.575×10^{-5}	0

Notice that the system presents a chaotic response that can be assured evaluating Lyapunov exponents. By employing the algorithm proposed by Wolf *et al.* [1985], one obtains the following spectrum that presents one positive value: $\lambda = \{+19.21, -5.19\}$.

4.1. *State space reconstruction*

This section analyzes state space reconstruction performed with the procedure of extended state observers. It is assumed a scalar time series associated with the pendulum position, $x_1 = \phi$, which is generated by numerical integration of the

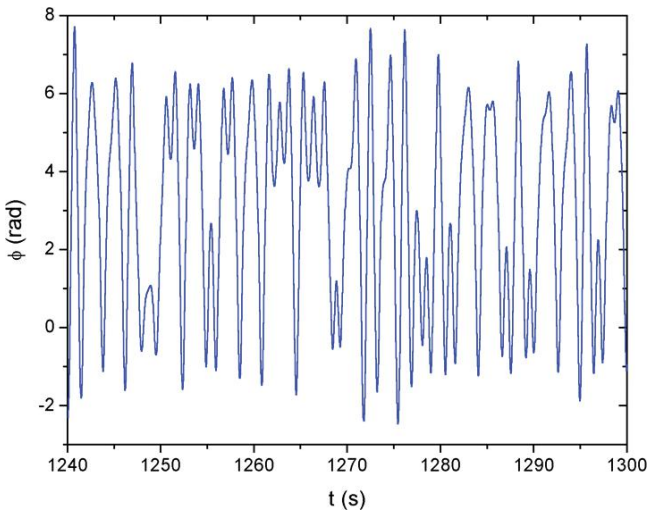

(a)

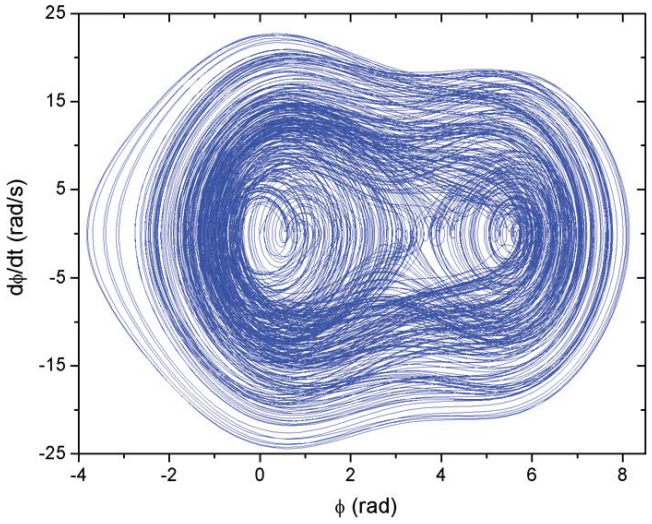

(b)

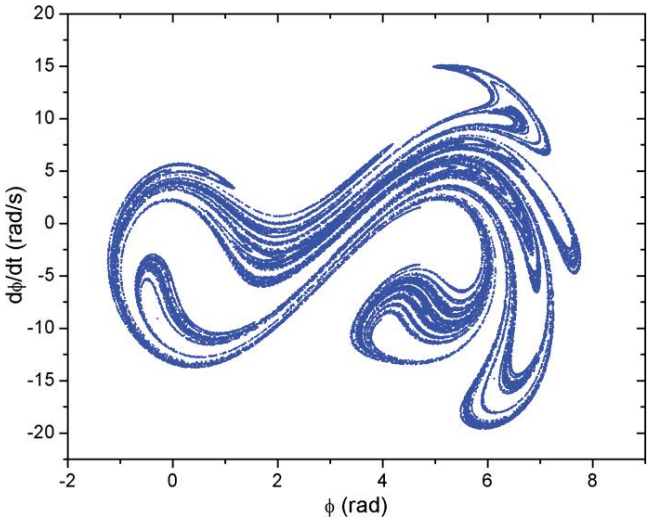

(c)

Fig. 2. Chaotic response. (a) Temporal evolution. (b) Phase space. (c) Strange attractor.

mathematical model. The reconstruction is done assuming a linear ESO where $g_i(e, \alpha_i, \delta) = e = x_1 - \hat{x}_1$ $(i = 1, 2, 3)$ in system (7).

In order to evaluate the sensitivity of the extended state observer procedure to the gain parameters, Fig. 3 shows different strange attractors related to the chaotic response of the pendulum. Different gain parameters are considered, imposing large variations of the bandwidth of the observer, ω_o: $\omega_o = 1$, $\omega_o = 10$, $\omega_o = 40$, $\omega_o = 80$. A comparison with the real attractor, obtained from all variables of the problem [Fig. 2(c)], shows that $\omega_o = 40$ presents an equivalent response. Therefore, it should be pointed out that the procedure presents a small sensitivity related to large variations of gain parameters. Great variations of the parameter ω_o do not alter the topological characteristic of the reconstructed attractor. Only $\omega_o = 1$ (40 times less than the ideal parameter) presents different results. Although the parameter ω_o is arbitrarily chosen here, there are procedures to perform an appropriated choice of this parameter. For details see [Gao, 2003].

The state space reconstruction using extended state observers has some advantages in chaos control. The method of delay coordinates, for example, leads to a map $F^{(n,n+1)}$ that will depend on all parametric changes that influence the system

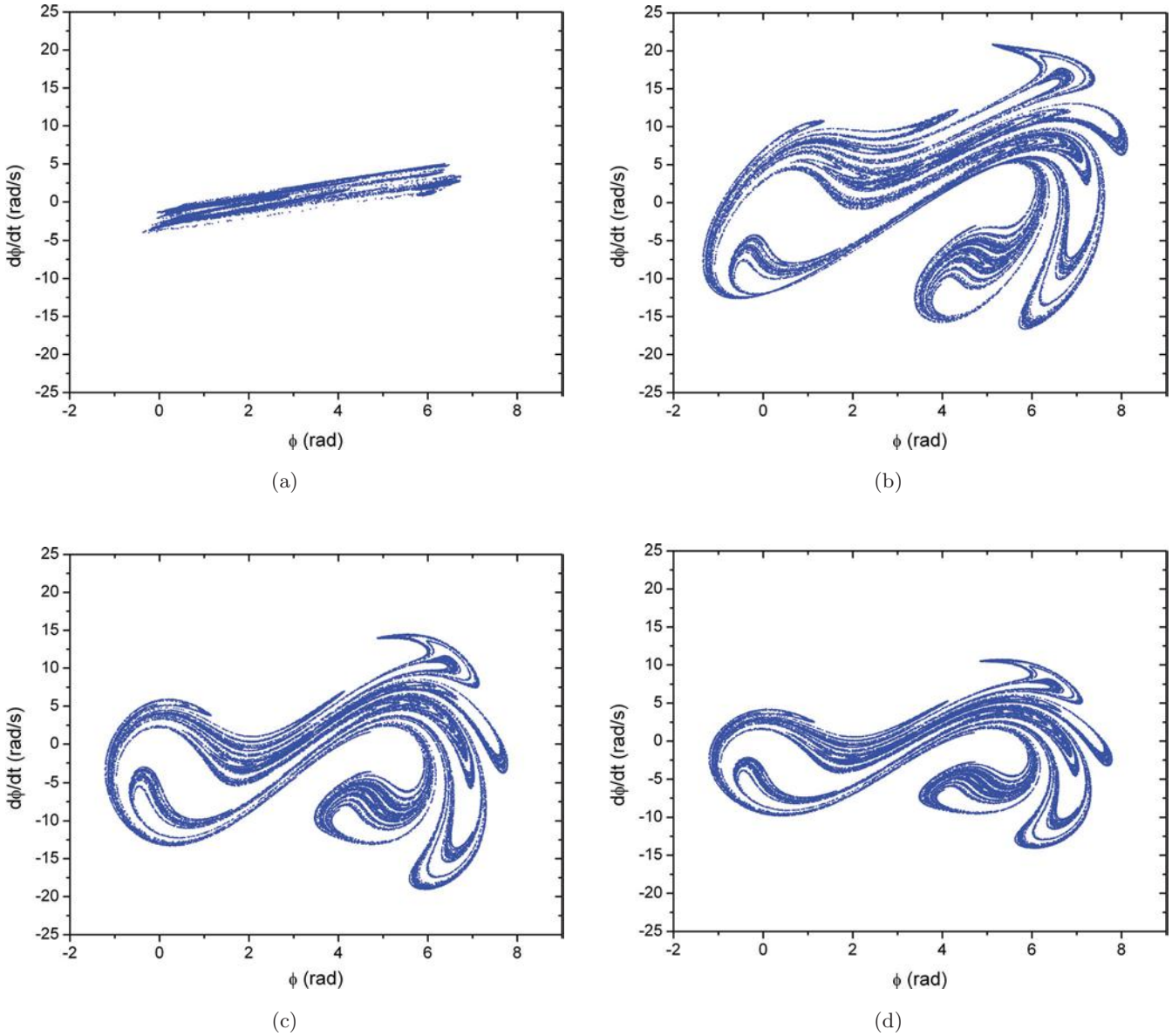

Fig. 3. Reconstructed attractors considering different parameters. (a) $\omega_o = 1$, (b) $\omega_o = 10$, (c) $\omega_o = 40$, (d) $\omega_o = 80$.

in the time interval $t^n - \tau \leq t \leq t^n$, that is, $\delta p^n, \delta p^{n-1}, \ldots, \delta p^{n-r}$ with r being the largest integer value such that δp^{n-r} lies in this interval [Pereira-Pinto *et al.*, 2004; Dressler & Nitsche, 1992]. Therefore, the use of extended state observers avoids these calculations, allowing a direct application of the SCC method.

5. Chaos Control

The first stage of the control strategy is the identification of UPOs embedded in the chaotic attractor. The CR method [Auerbach *et al.*, 1987] is employed with this aim assuming a tolerance $r_1 = 0.006\pi$ while r_2 is set to be ten times r_1. Figure 4 presents a strange attractor of the motion showing points in the Poincaré section #1 corresponding to some identified UPOs that will be stabilized in the next stage of control strategy. The application of the SCC method considers three control stations (named intermediate Poincaré section #2, #3, #4, Fig. 5). Therefore, a total of four maps per forcing period are considered.

After the identification of the UPOs embedded in the Poincaré section #1, the piercing of the same UPOs in the other three Poincaré sections is determined. Then, the local dynamics expressed by the Jacobian matrix and the sensitivity vector of the transition maps in a neighborhood of the fixed points are determined using the least-square fit method [Auerbach *et al.*, 1987; Otani & Jones, 1997]. After that, the SVD technique is employed

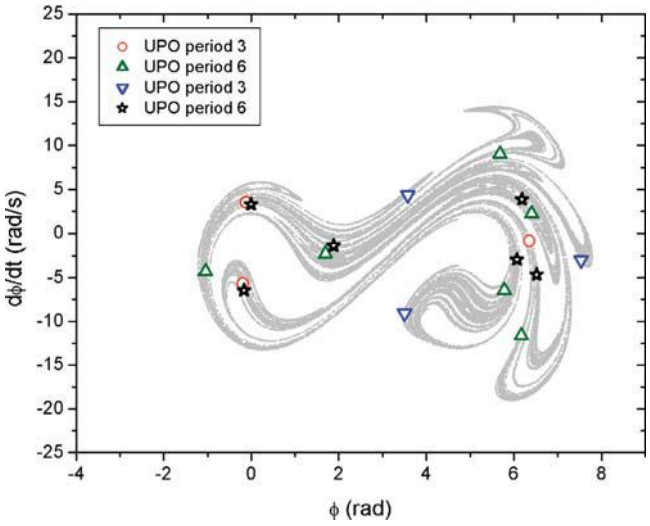

Fig. 4. Unstable periodic embedded in the attractor.

for determining the stable and unstable directions near the next fixed point. The sensitivity vectors are evaluated allowing the trajectories to come close to a fixed point and then one perturbs the parameters by the maximum permissible value. In this case, it is assumed a perturbation $\Delta l_{\max} = 20\,\text{mm}$, fitting the resulting deviations $[\delta\xi^{n+1}(\Delta l) - A^n \delta\xi^n]/\Delta l$ from the next piercing by the least square procedure. After that, SCC method is employed to stabilize unstable periodic orbits and the parameter changes are calculated from Eq. (5).

The stabilization of UPOs is simulated considering the following sequence: during the first 500 forcing periods control is off. After that, it is

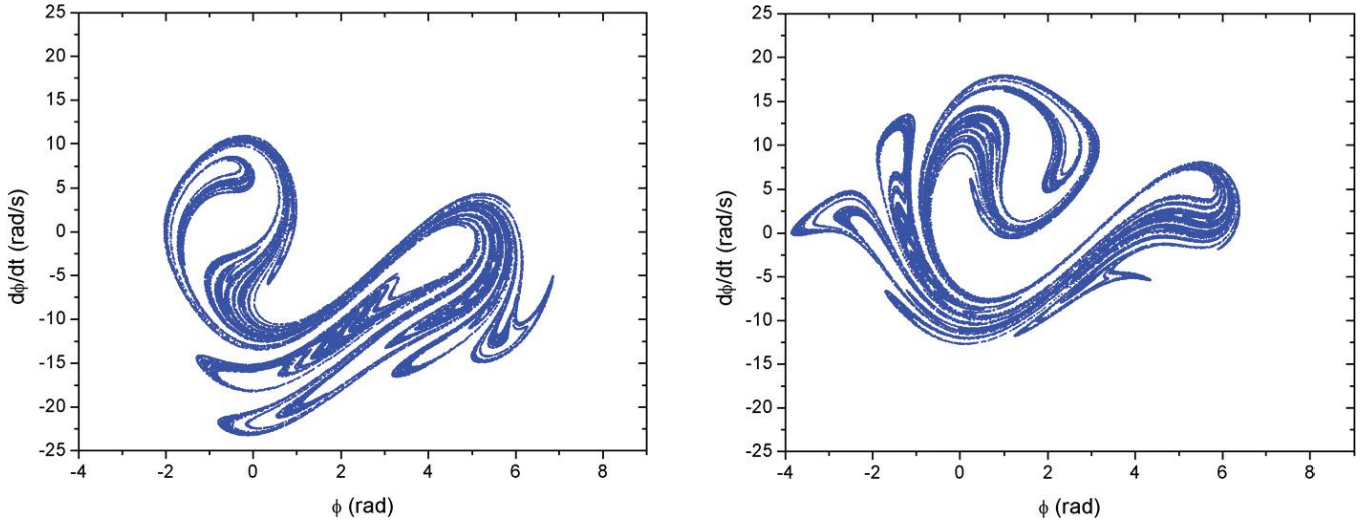

(a) (b)

Fig. 5. (a) Poincaré map #2, (b) Poincaré map #3, (c) Poincaré map #4.

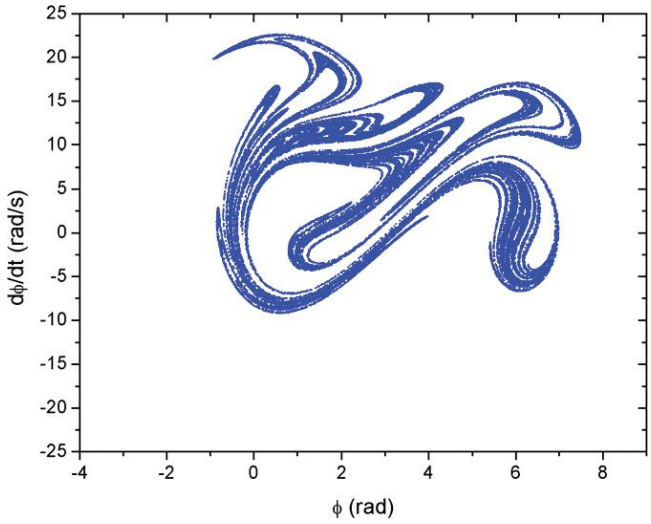

(c)

Fig. 5. (*Continued*)

stabilized at period-3 UPO between 500 and 1000 forcing periods. A period-6 UPO is then stabilized between 1000 and 1500 forcing periods. Afterwards, it is stabilized at period-3 UPO, different from the first one, between 1500 and 2000 forcing periods and finally at period-6, from 2000 and 2500 forcing periods. Figure 6 shows the system's dynamics in the Poincaré section #1 during this sequence of actuation. Notice that different times are needed for the system to achieve the desired stabilization on a particular UPO. This happens because one must wait until the trajectory comes close enough to a control point to perform the necessary perturbation, exploiting the ergodicity property of chaos. Moreover, it should be pointed out that, as expected, results show that unstable orbits are stabilized with small variations of control parameter after a transient, less than 10 mm in this case.

Figures 7–10 show details on stabilized orbits. Phase space, time evolution of position and control parameters are presented. Moreover, a comparison between the unstable periodic orbit stabilized using conventional control (all state variables are available) and observer-based control are shown, presenting good agreements.

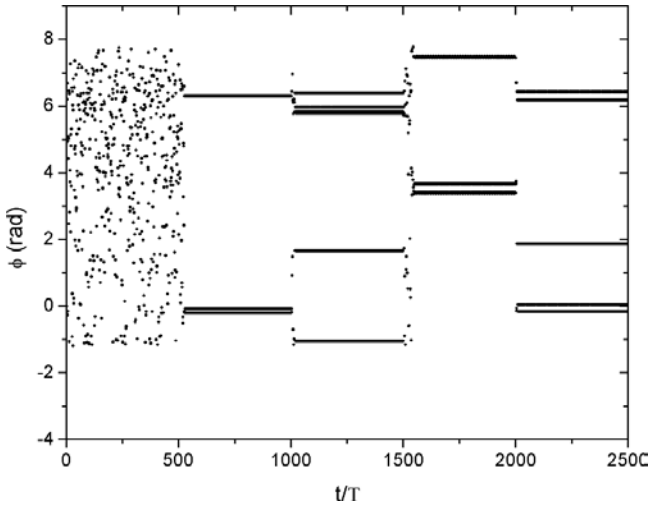

(a)

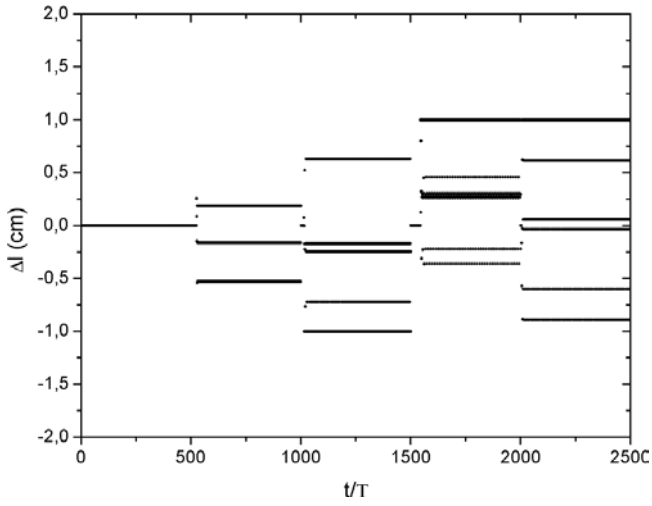

(b)

Fig. 6. Response under control. (a) Temporal alternating of UPOs in Poincaré section #1. (b) Control signal.

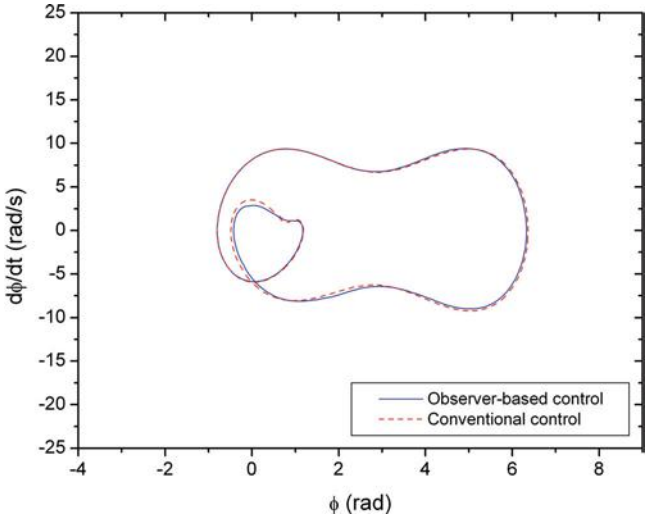

(a)

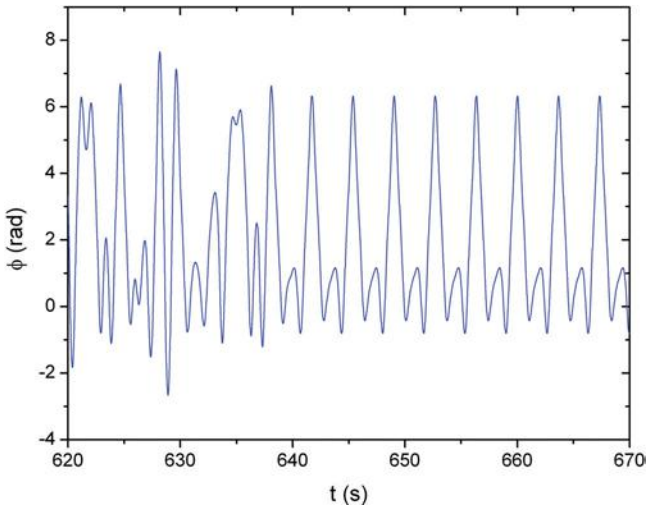

(b)

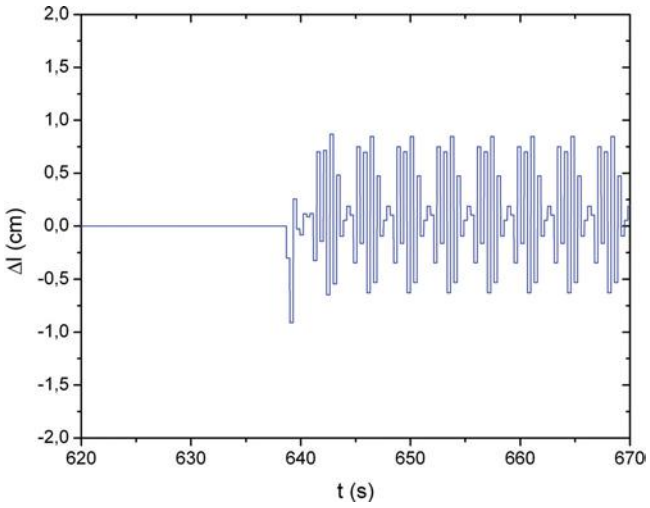

(c)

Fig. 7. Period-3 UPO.

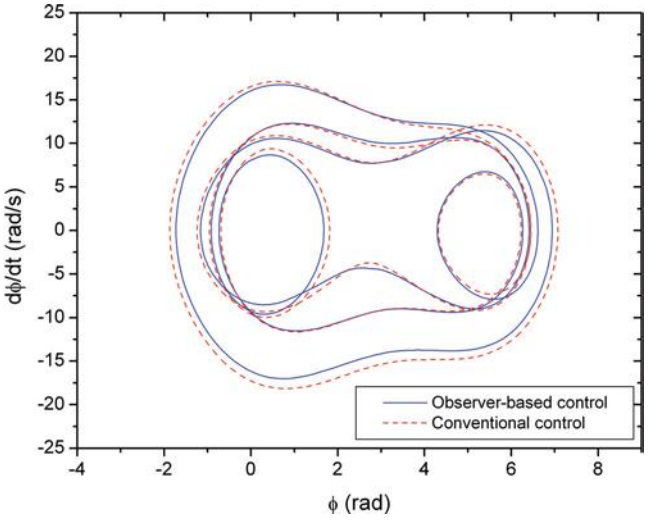

(a)

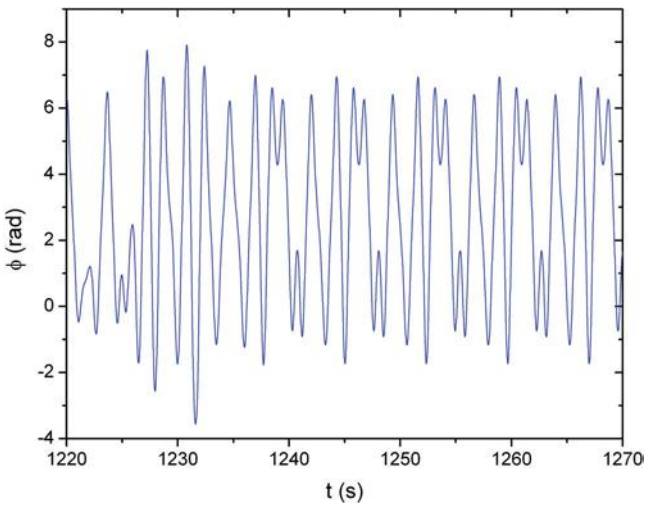

(b)

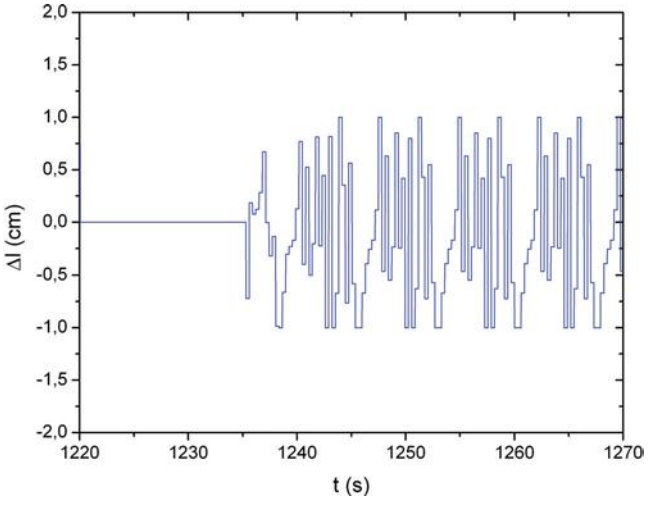

(c)

Fig. 8. Period-6 UPO.

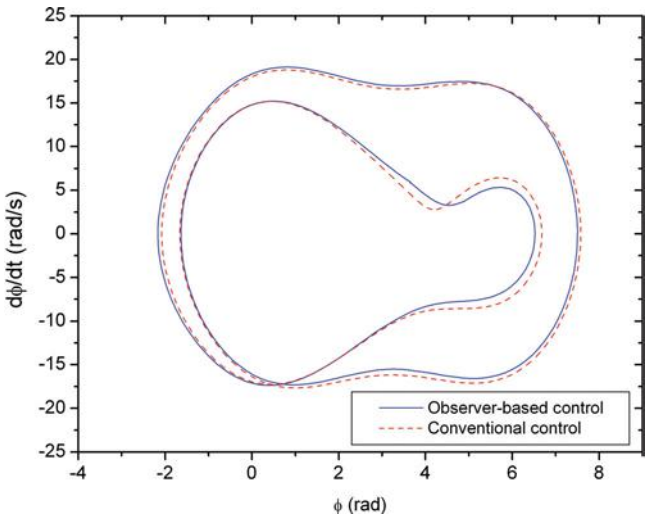

(a)

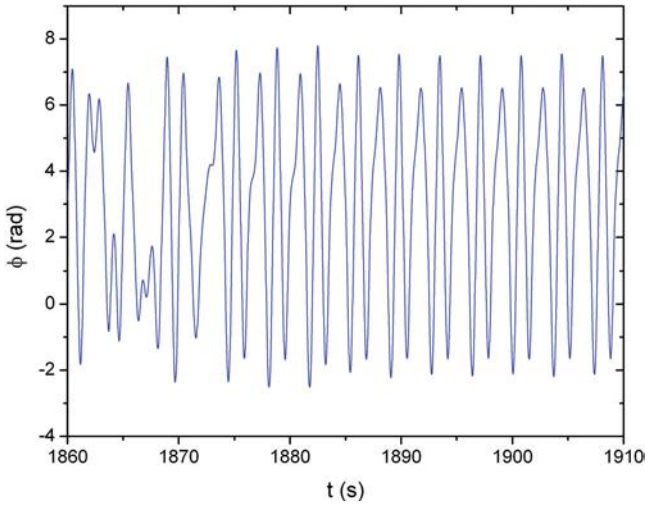

(b)

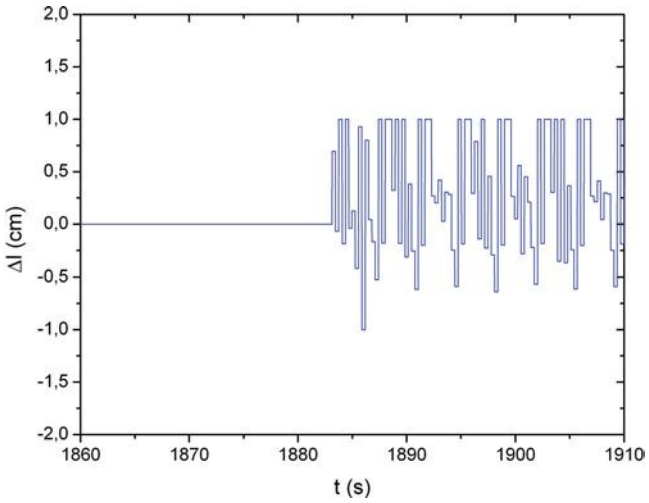

(c)

Fig. 9. Period-3 UPO.

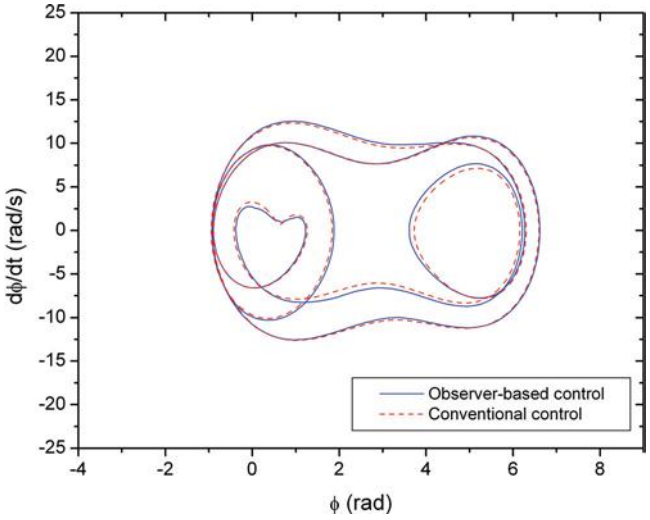

(a)

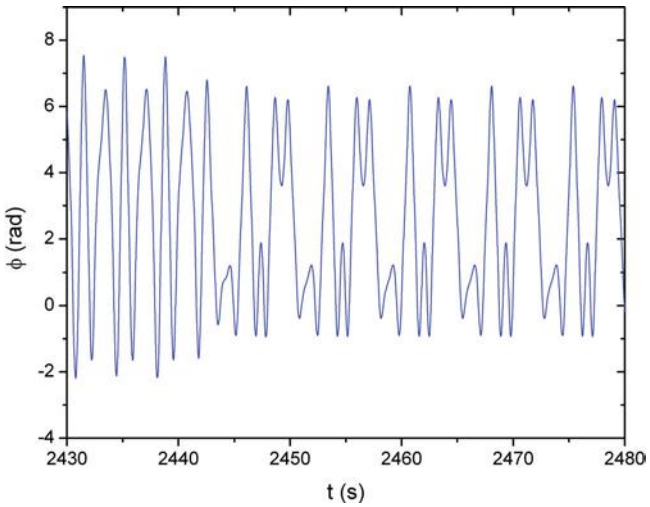

(b)

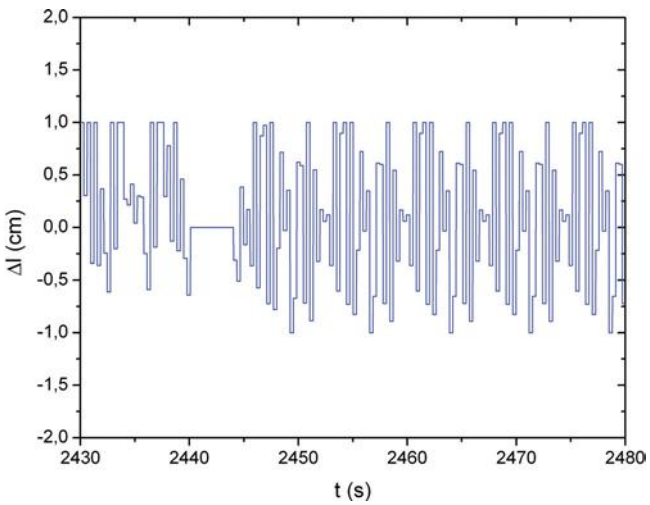

(c)

Fig. 10. Period-6 UPO.

6. Conclusions

This contribution discusses the state space reconstruction using extended state observers applied to the control of chaos in a simulated nonlinear pendulum. The use of extended state observers showed to be effective in order to perform reconstruction. In terms of control strategy, the first stage uses the close-return method to identify unstable periodic orbits (UPOs) embedded in the chaotic attractor. After that, the semi-continuous control (SCC) method is considered to stabilize desirable orbits. Least-square fit method is employed to estimate Jacobian matrixes and sensitivity vectors. Moreover, SVD decomposition is employed to estimate directions of unstable and stable manifolds in the vicinity of control points. The use of extended state observers allows a direct application of a SCC method. Compared with delay coordinate method, this procedure avoids the calculation of parametric changes related to delayed Poincaré sections. Simulations of control procedure show that SCC method is capable to perform stabilization of the nonlinear pendulum.

Acknowledgment

The authors acknowledge the support of the Brazilian Research Council CNPq.

References

Auerbach, D., Cvitanovic, P., Eckmann, J.-P., Gunaratne, G. & Procaccia, I. [1987] "Exploring chaotic motion through periodic orbits," *Phys. Rev. Lett.* **58**, 2387–2389.

Bowong, S. & Kakmeni, F. M. M. [2003] "Chaos control and duration time of a class of uncertain chaotic systems," *Phys. Lett.* **A316**, 206–217.

Broomhead, D. S. & King, G. P. [1986] "Extracting qualitative dynamics from experimental data," *Physica* **D20**, 217–236.

Cao, Y. J. [2000] "A nonlinear adaptative approach to controlling chaotic oscillators," *Phys. Lett.* **A270**, 171–176.

Dressler, U. & Nitsche, G. [1992] "Controlling chaos using time delay coordinates," *Phys. Rev. Lett.* **68**, 1–4.

Femat, R., Ramírez, J.-A. & González, J. [1997] "A strategy to control chaos in nonlinear driven oscillators with least prior knowledge," *Phys. Lett.* **A224**, 271–276.

Franca, L. F. P. & Savi, M. A. [2001] "Distinguishing periodic and chaotic time series obtained from an experimental nonlinear pendulum," *Nonlin. Dyn.* **26**, 253–271.

Gao, Z., Huang, Y. & Han, J. [2001] "An alternative paradigm for control system design," *IEEE Conf. Decision and Control*.

Gao, Z. [2003] "Scaling and bandwidth-parameterization based controller tuning," in *American Control Conf.*, Denver, Colorado.

Gunaratne, G., Linsay, P. S. & Vinson, M. J. [1989] "Chaos beyond onset: A comparison of theory and experiment," *Phys. Rev. Lett.* **63**, 1–4.

Han, J. [1995] "A class of extended state observers for uncertain systems," *Contr. Decis.* **10**, 85–88.

Hübinger, B., Doerner, R., Martienssen, W., Herdering, M., Pitka, R. & Dressler, U. [1994] "Controlling chaos experimentally in systems exhibiting large effective Lyapunov exponents," *Phys. Rev.* **E50**, 932–948.

Kalman, R. E. [1960] "A new approach to linear filtering and prediction problems," *Trans. ASME — J. Basic Engin.* **D82**, 35–45.

Korte, R. J. de, Schouten, J. C. & van den Bleek, C. M. V. [1995] "Experimental control of a chaotic pendulum with unknown dynamics using delay coordinates," *Phys. Rev.* **E52**, 3358–3365.

Luenberger, D. G. [1964] "Observing the state of a linear system," *IEEE Trans. Milit. Electron.* v.MIL 8.

Luenberger, D. G. [1966] "Observers for multivariable systems," *IEEE Trans. Autom. Contr.* **AC 11**.

Otani, M. & Jones, A. J. [1997] "Guiding chaotic orbits," 130, Research Report — Imperial College of Science Technology and Medicine, London.

Ott, E., Grebogi, C. & Yorke, J. A. [1990] "Controlling chaos," *Phys. Rev. Lett.* **64**, 1196–1199.

Packard, N. J., Crutchfield, J. P., Fromer, J. D. & Shaw, R. S. [1980] "Geometry from a time-series," *Phys. Rev. Lett.* **45**, 712–716.

Pereira-Pinto, F. H. I., Ferreira, A. M. & Savi, M. A. [2004] "Chaos control in a nonlinear pendulum using a semi-continuous method," *Chaos Solit. Fract.* **22**, 653–668.

Pinto, E. G. F. & Savi, M. A. [2003] "Nonlinear prediction of time series obtained from an experimental pendulum," *Current Topics in Acoustical Research — Research Trends*, Vol. 3, pp. 151–162.

Pyragas, K. [1992] "Continuous control of chaos by self-controlling feedback," *Phys. Lett.* **A170**, 421–428.

Ramirez, J.-A. & Villamil, F.-V. [1995] "State estimation for a class of nonlinear oscillators with chaotic attractor," *Phys. Lett.* **A197**, 116–120.

Ruelle, D. [1979] "Ergodic theory of differentiable dynamical systems," *Mathématique of the Institut des Hautes Études Scientifiques*, Vol. 5, pp. 27.

So, P., Ott, E. & Dayawansa, W. P. [1994] "Observing chaos: Deducing and tracking the state of a chaotic

system from limited observation," *Phys. Rev.* **E49**, 2650–2660.

Takens, F. [1981] "Detecting strange attractors in turbulence," in *Proc. Symp. Dynamical Systems and Turbulence*, University of Warwick, 1979–1980, eds. Rand, D. A. & Young, L. S. (Springer, Berlin).

Wang, W. & Gao, Z. [2003] "A comparison study of advanced state observer design techniques," in *American Control Conf.*, Denver, Colorado, June.

Wolf, A., Swift, J. B., Swinney, H. L. & Vastano, J. A. [1985] "Determining Lyapunov exponents from a time series," *Physica* **D16**, 285–317.